E3S Web of Conferences **417**, 05009 (2023) https://doi.org/10.1051/e3sconf/202341705009
GEOTECH-2023

Construction of continuous and discrete non-linear prognostic models of the control system for the process of grinding ore materials

Djalolitdin Mukhitdinov[1], *Sanjar* Boybutayev[2*], *Olmosjon* Goziev[2], and *Javohir* Qudratov[2]

[1]Tashkent State technical University, Electronics and automatical faculty, Tashkent, 100095, Uzbekistan
[2]Navoi State University of Mining and Technologies, Department of Automation and Control, Energy-mechanics faculty, Navoi, 210100, Uzbekistan

Abstract. The article analyzes the developed non-linear predictive model of the control system in continuous time of the state space, including states, control and controlled values. The transformation of the continuous form of a function into a discrete one is carried out according to the trapezoid rule. Based on the discrete model, the optimality criterion for the objective function is formulated. The efficiency of the grinding process is considered based on the weight components of the model, since it entirely depends on the accuracy of estimating the particle size of the product and the performance of the plant. To control the volume of water in the sump, a dynamic inversion controller is provided, which makes it possible to reduce control problems to a solution in a closed form and guarantee asymptotic stability of the error dynamics.

1 Introduction

The nonlinear predictive model of the control system in continuous time of the state space can be represented as the following functional dependencies:

$$\dot{z}_d(\tau) = f_d(\tau, z_d, c_d) \quad (1)$$

$$F_d(\tau) = g_d(\tau, z_d, c_d) \quad (2)$$

where: z_d corresponds to state variables, F_d corresponds to output measured variables, and c_d - managed object variables. States, controlled and measured quantities can be represented as the following relationships:

$$z_d = [Z_{mw}, Z_{ms}, Z_{mf}, Z_{mr}, Z_{mb}, Z_{ss}, Z_{sf}]^T \quad (3)$$

$$c_C = [RWF, \mathrm{AOFM}, \mathrm{ABFM}, \alpha_{\mathrm{speed}}, \mathrm{RFC}, Z_{\mathrm{sw}}]^T \quad (4)$$

$$F_C = [\mathrm{LOAD}, \mathrm{SFP}, \mathrm{P}]^T \quad (5)$$

where: Z_{mw}, Z_{ms}, Z_{mf}, Z_{mr}, Z_{mb} - volume of mill water, solids, fines, stones and balls in the mill respectively;

Z_{sw}, Z_{ss}, Z_{sf} - volumes of water, solids and fines in the sump;

RWF - Rate of water flow into the mill;

* Corresponding author: sboybutayev@mail.ru

AOFM - The amount of ore that feed into mill;
ABFM- The amount of balls that feed into mill;
α_{speed} - The percentage of the mill's critical rotational speed;
RFC - The rate of flow into cyclone;
LOAD - The percentage of the mill's total volume;
P - the percentage of productivity of grinding process;
SFP - the size distribution of particles in the final product;

The time range from the amount of ore that feed into mill (AOFM) to the size distribution of particles in the final product (SFP) is 30 minutes, and the rate of flow into cyclone (RFC) to RFC is 2 minutes. In addition, the technological process in the mill is quite slow compared to the process in the sump. For example, with a difference in the flow rates of the SFP and rate of water flow into the mill (RWF) of 400 m^3/h, the slurry located in the sump with a volume of 15 m^3 can pass through it within 1 min. [1-4].

Since the processes proceeding quickly and slowly can be depicted in the diagram as two separate circuits: a) – including an auxiliary low speed controller used for the sump, and - b) including the main controller used for the rest of the circuit, designed for optimization and carrying a large data processing load.

2 Materials and methods

Let's build the architecture for controlling the grinding process in a ball mill. Schematic control of the mill is shown in Figure 1.

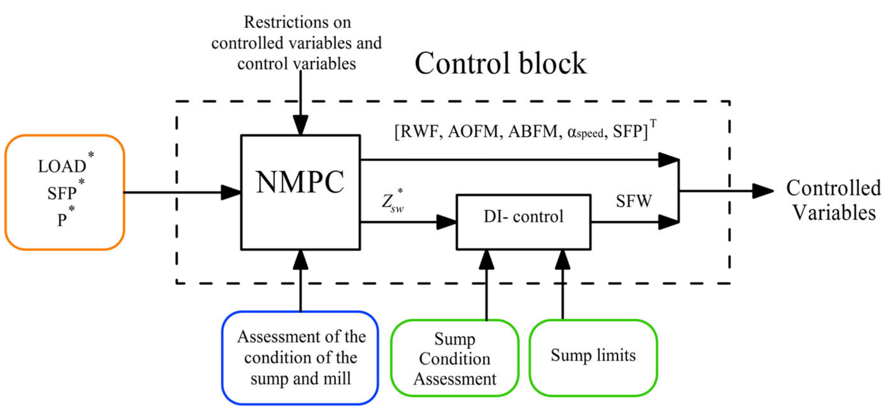

Fig. 1. Grinding process control scheme.

where – SFW - Sump feed water flow-rate

The grinding process control scheme shown in Figure 1, consists of a dynamic DI inversion control loop, and a loop combined with a non-linear model. The dynamic inversion controller (DI) is designed to control the process occurring in the sump. This allows the nonlinear model to more accurately determine the optimal values of the remaining variables. Unlike two isolated controllers, the predictive control system model generates a single solution, given the solution generated by the dynamic inversion (DI) controller.

Function f_d is determined from the formulas [1-8] (6) - (13):

$$\dot{Z}_{\text{mw}} = RWF - (\phi V_v Z_{\text{mw}} Z_{\text{mw}})/(Z_{\text{ms}} + Z_{\text{mw}}) + V_{\text{cwu}} \quad (6)$$

$$\dot{Z}_{\text{ms}} = \text{AOFM}/\rho_b(1-\alpha_r) - (\phi V_v Z_{\text{mw}} Z_{\text{ms}})/(Z_{\text{ms}} + Z_{\text{mw}}) + V_{\text{csu}} + \\ +(\phi P_{\text{mill}})/(\rho_b \phi_r) \cdot Z_{\text{mr}}/(Z_{\text{mr}} + Z_{\text{ms}}) \quad (7)$$

$$\dot{Z}_{\text{mf}} = (\text{AOFM})/\rho_b \cdot \alpha_f - (\phi V_v Z_{\text{mw}} Z_{\text{mf}})/(Z_{\text{ms}} + Z_{\text{mw}}) + V_{\text{cfu}} + \\ +(\phi P_{\text{mill}})/(\rho_b \varphi_f)/[1 + \alpha_{\varphi f} \cdot ((Z_{\text{mw}} + Z_{\text{mr}} + Z_{\text{ms}} + Z_{\text{mb}})/(v_{\text{mill}}) - v_{P_{max}} \quad (8)$$

$$\dot{Z}_{\mathrm{mr}} = (\mathrm{AOFM})/\rho_b \cdot \alpha_r - (\phi P_{\mathrm{mill}})/(\rho_b \varphi_r)(Z_{\mathrm{mr}}/(Z_{\mathrm{mr}} + Z_{\mathrm{ms}})) \quad (9)$$

$$\dot{Z}_{\mathrm{mb}} = (\mathrm{ABFM})/\rho_s - (\phi P_{\mathrm{mill}})/\varphi_b (Z_{\mathrm{mb}}/(\rho_b (Z_{\mathrm{mr}} + Z_{\mathrm{ms}}) + \rho_s Z_{mb})) \quad (10)$$

$$\dot{Z}_{\mathrm{sw}} = (\phi \cdot V_v \cdot Z_{\mathrm{mw}} \cdot Z_{\mathrm{mw}})/(Z_{\mathrm{ms}} + Z_{\mathrm{mw}}) - (RFC \cdot Z_{\mathrm{sw}})/(Z_{\mathrm{sw}} + Z_{\mathrm{ss}}) + SFW \quad (11)$$

$$\dot{Z}_{\mathrm{ss}} = (\phi \cdot V_v \cdot Z_{\mathrm{mw}} \cdot Z_{\mathrm{ms}})/(Z_{\mathrm{ms}} + Z_{\mathrm{mw}}) - (RFC \cdot Z_{\mathrm{ss}})/(Z_{\mathrm{sw}} + Z_{\mathrm{ss}}) \quad (12)$$

$$\dot{Z}_{\mathrm{sf}} = \frac{\phi \bullet V_v \bullet Z_{\mathrm{mw}} \bullet Z_{\mathrm{mf}}}{Z_{\mathrm{ms}} + Z_{\mathrm{mw}}} - \frac{RFC \bullet Z_{\mathrm{sf}}}{Z_{\mathrm{sw}} + Z_{\mathrm{ss}}} \quad (13)$$

Function g_d is determined by the formulas [2]: (14) - (18)

$$LOAD = (Z_{\mathrm{mw}} + Z_{\mathrm{ms}} + Z_{\mathrm{mr}} + Z_{\mathrm{mb}})/\upsilon_{\mathrm{mill}} \quad (14)$$

$$SLEV = Z_{\mathrm{ss}} + Z_{\mathrm{sw}} \quad (15)$$

$$SFP = V_{\mathrm{cfo}}^{''}/V_{\mathrm{cso}}^{''} \quad (16)$$

$$P = V_{\mathrm{cso}}^{''} \quad (17)$$

$$P_{\mathrm{mill}} = P\{1 - \delta_{p\vartheta} Z_x^2 - 2\chi_{\max}\delta_{p\vartheta}\delta_{ps} Z_x Z_r - \delta_{ps} Z_r^2\}_{\mathrm{speed}}{}^{\alpha_p}{}_{max} \quad (18)$$

To transform the continuous form of the function f_C into a discrete one, we use the trapezoid rule:

$$z_{k+1} = z_k + \frac{1}{2}\hbar[f_d(\tau(k+1), z_d, c_d) + f_d(\tau(k), z_d, c_d)] \quad (19)$$

where $\hbar$ — step size.

We will solve the equation with respect to z_{k+1}. To obtain a solution, we use the Newton-Raphson method. The transformed equation takes the following form:

$$z_{k+1}^i = \mathbf{z}_{k+1}^{i-1} + \left[I - \frac{1}{2}\frac{\partial f_{\mathbf{d}}}{\partial z}|z_{k+1}, \mathrm{c}_{k+1}\right]^{-1} \psi(z_{k+1}^{i-1}, z_k, \mathrm{c}_{k+1}, c_k) \quad (20)$$

In the equation (20) i - iteration index. The last component of equation (20) is determined from the relation:

$$\psi(z_{k+1}^{i-1}, z_k, \mathrm{c}_{k+1}, c_k) = z_{k+1} - z_k - \frac{1}{2}\hbar[f_d(\tau(k+1), z_d, c_d) + f_d(\tau(k), z_d, c_d)] \quad (21)$$

A discrete model of a control system in a nonlinear state space can be represented as the following relations:

$$z_{k+1} = f_{d_k}(z_k, c_k) \quad (22)$$

$$F_k = g_{d_k}(z_k, u_k) \quad (23)$$

From the equation (22-23) of the discrete model, it is possible to formulate the optimality criterion for the target function, which minimizes the function (24):

$$\begin{aligned} &\min_{\mathrm{u}_k,\ldots\mathrm{u}_{k+N_C-1}} J(\mathrm{c}_k,\ldots,\mathrm{c}_{k+N_C-1},\mathrm{z}_k) \\ \text{s.t.} \quad & \mathrm{z}_{k+1} = \mathrm{f}_{d_k}(\mathrm{z}_k,\mathrm{c}_k) \\ & \mathrm{F}_k = \mathrm{g}_{d_k}(\mathrm{z}_k,\mathrm{c}_k) \\ & \mathrm{c}_l \le \mathrm{c}_k \le \mathrm{c}_u \\ & \Delta\mathrm{c}_l \le \Delta\mathrm{c}_k \le \Delta\mathrm{c}_u \\ & \mathrm{F}_l \le \mathrm{F}_k \le \mathrm{F}_u \end{aligned} \quad (24)$$

In equation (24), the target function J is determined from the expression:

$$J(\cdot) = \sum_{i=0}^{N_P-1}(F_{sp} - F_{k+i|k} + D)^T Q_1 (F_{sp} - F_{k+i|k} + D) + \sum_{i=0}^{N_C-1}(\Delta c_{k+i|k})^T Q_2 (\Delta c_{k+i|k}) \quad (25)$$

where F_{sp} – set-points for controlled variable, Np – maximum predicted values, and Nc – maximum control values, Q_1 and Q_2 – are arbitrary matrices.

Arbitrary matrices are used to transform state equations. Let us assume that the system is described by the general equations of state $\dot{z} = Az + Bv$, $F = Cz$. If we make the following substitution z=Qw, you can get a new state vector $w = col[w_1, \ldots, w_n]$. Q – an arbitrary matrix of dimension with constant coefficients, on which the only restriction is imposed - its determinant must not be equal to zero. If this condition is met, we can find the inverse matrix

Q^{-1} such that $Q^{-1}Q = E$. In this case, we can assert the existence of a one-to-one relationship between the vectors *z* and *w*: $z = Qw$, $w = Q^{-1}z$.

After replacing $z = Qw$ in the general equation of state $\dot{z} = Az + Bv$ and, given that $\dot{z} = Q\dot{w}$, you can get new equations $\dot{w} = Q^{-1}AQw + Q^{-1}B$v, $F = CQw$, which are new equations of state. The resulting two matrices A and A_1 are similar.

Similar matrices have the same eigenvalues. It is possible to select a certain type of equation of state when conducting a study by the method of linear transformation. In most cases, the problem is solved by replacing the original system with the normal or canonical form of the equations of state. It is known that for an arbitrary matrix *A* there exists a square matrix of size *nxn*, and this square matrix is called a modal matrix *M*. If an arbitrary matrix has an eigenvalue whose characteristic equation has roots equal to $\lambda_1, \ldots, \lambda_n$, a $det[A - \lambda E] = 0$ satisfy this condition, then the matrix $M^{-1}AM$ is diagonal, i.e. $M^{-1}AM = diag[\lambda_1, \ldots, \lambda_n]$. This, the system of arbitrary equations can be reduced to the canonical form [9-14].

The constant *D* in equation (25) is determined from the difference between the measured value at the output of the object and the value of this value calculated by the model $D = \hat{F}_k - F_k$ in τ(k), which is the result of additive step disturbances that persist throughout the entire predicted interval [15-20].

Despite its simplicity, this method has the advantage of being able to accurately model the "set-point" changes entering the feedback loop as step disturbances and to approximate slowly varying discrepancies between the modeled data and the zero correction for step changes "set-point". However, the accuracy of the values obtained by this method can be affected by random fluctuations in the output signal.

Due to the possibility of the emergence of competitive and conflicting goals, the formulation of the predictive model of the control system does not provide for restrictions on the input conditions.

In steady state, the performance of the mill corresponds to the consumption the amount of ore that feed into mill (AOFM). Provided the ore feed is stabilized and the size distribution of particles in the final product (SFP) is maintained at an elevated level, the percentage of productivity of grinding process (P) can be increased. In this case, a decrease in the supply of ore will prevent an increase in productivity, because. In steady state, according to the material balance, the amount of input is equal to the amount of output. Such a phenomenon can cause a decrease in the rate of change of the controlled variables, which can lead to an increase in energy costs for making corrections to the values of the controlled variables. To prevent such cases and maintain the scheme in the workspace, upper and lower limit values for controlled (F_u, F_l) and controlled variables (c_u, c_l). These values are shown in Table 1.

Provided that the values of controlled and controlled variables are within the specified boundaries, the states will also be within the working boundaries. On this basis, restrictions on states are not included in the mathematical description of the model. The tuning parameters of the nonlinear model are the weight matrices of the controlled variables Q_1 and Q_2 - rate of change of control variables.

Table 1. Input parameters, upper and lower limit values for monitored and controlled variables, and speed limits.

Var	Value	Min	Max	Δ	Unit
		Manipulated variables			
RWF	7.12	0	40	2	[m³/h]
AOFM	82	0	120	1	[t/h]
ABFM	6.5	0	10	0.5	[t/h]
α_{speed}	0.71	0.6	0.8	0.01	[-]
RFC	650	400	850	5	[m³/h]
SFW	300	0	500	-	[m³/h]

		Measured variables			
LOAD	0.42	0.3	0.45	-	[-]
SFP	0.7	0.65	0.80	-	[-]
P	20.8	15	30	-	[m^3/h]
SLEV	10	2	15	-	[m^3]
P_{mill}	3445	-	-	-	[kW]
CFD	1.81	-	-	-	[t/m^3]
		States			
Z_{mw}	4.80	-	-	-	[m^3]
Z_{ms}	4.85	-	-	-	[m^3]
Z_{mf}	1.04	-	-	-	[m^3]
Z_{mr}	1.77	-	-	-	[m^3]
Z_{mb}	8.01	-	-	-	[m^3]
Z_{sw}	4.06	2	15	-	[m^3]
Z_{ss}	1.83	-	-	-	[m^3]
Z_{sf}	0.42	-	-	-	[m^3]

3 Results

Consider the efficiency of the grinding process, based on the weight components of the model. The economic efficiency of the grinding scheme depends on the accuracy of the product particle size estimation and throughput. Therefore, it is necessary to exercise more careful control over the control of these parameters in comparison with the parameter corresponding to the filling fraction of the mill.

On this basis, the weight matrix $Q_1=\text{diag}\{q_{11}, q_{12}, q_{13}\}$, corresponding to the output variables, is drawn up so that the deviation of the measured values of productivity from the "set-point" by 0.5% will lead to an error equal to the PSE from the given "set-point" by 1% when calculating the costs. In this case, the deviation of the mill filling fraction from the "set-point" will be 10%.

Mathematically, this can be expressed as the relation (26)

$$q_{11}(10\%LOAD_{SP})^2 = q_{12}(0.5\%P_{SP})^2 = q_{13}(1\%SFP_{SP})^2 \tag{26}$$

Weight matrix $Q_2=\text{diag}\{q_{21}, q_{22}, \ldots, q_{26}\}$, corresponding to the input variables is designed so that a 1% change in half the range corresponding to the flow rate of the circulating mixture and the volume of water in the sump will give the same error as a 2% change in half the range of water and ore supply to the mill, or 15% change in mill engine speed.

Since the change in the speed of the mill motor and the number of steel balls significantly affect the energy consumption, it is necessary to minimize them to values corresponding to the given productivity.

To prevent the possible washing out of fine particles from the mill, one should not sharply increase the flow of water to the mill, especially since this can lead to a rapid drop in the power consumption of the mill.

The paper [3] provides data that effective control of water flow into the mill allows one to determine the optimal control range for estimating the particle size of the finished product.

The matrix of input weights is represented as a ratio (27)

$$\begin{aligned} &q_{21}(2\%RWF_{range}/2)^2 = q_{22}(2\%AOFM_{range}/2)^2 = q_{23}(15\%ABFM_{range}/2)^2 \\ &= q_{24}(15\%{\alpha_{speed}}_{range}/2)^2 = q_{25}(1\%RFC_{range}/2)^2 = q_{26}(1\%{Z_{sw}}_{range}/2)^2 \end{aligned} \tag{27}$$

After appropriate transformations, equation (27) is transformed to the form:

$$q_{21}(2\%RWF_{range}/2)^2 = 100q_{11}\frac{N_P}{N_C}(10\%LOAD_{SP})^2 \tag{28}$$

Consider the operation of the dynamic inversion controller (DI), designed to control the process occurring in the sump.

The dynamic inversion controller controls the volume of water in the sump. Digital input control works on the principle that PID control is implemented as a stable linear system. After selecting the controller, the value of the control signal is calculated by inverting the dynamics of the system.

When non-linear system dynamics are available, the implementation of a dynamic controller inversion is preferable to the implementation of a PID controller. This is explained by the fact that the dynamic inversion method reduces to solving the control problem in a closed control form and guarantees the asymptotic stability of the error dynamics.

Dynamic inversion makes it possible to obtain the required response trajectory of the system by selecting the values of the proportional and integral gains such that

$$eK_P + K_I \int_0^t e d\tau + \dot{e} = 0 \tag{29}$$

where $e = \hat{F} - F_{sp}$ - difference between measured ($\hat{F}$) and set value (F_{sp}).

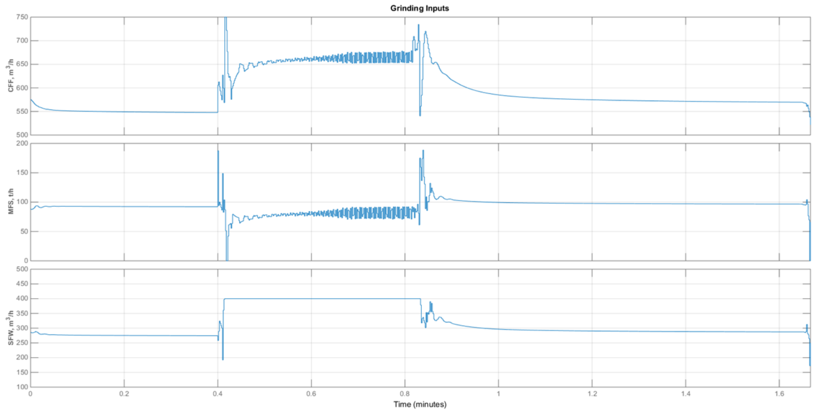

Fig. 2. Graph of the input parameters of the grinding process.

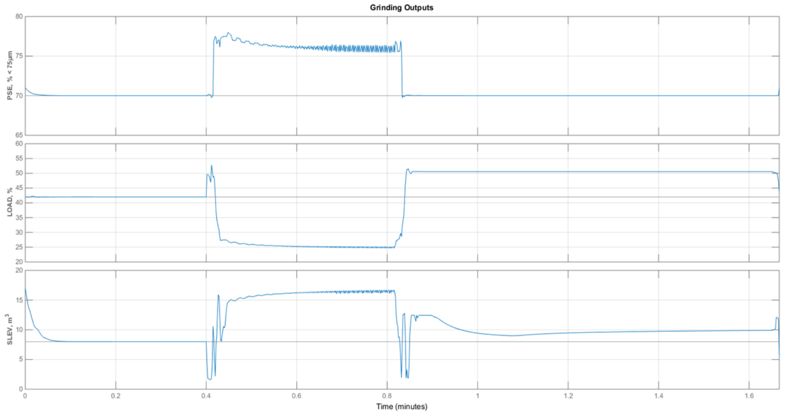

Fig. 3. Graph of the output parameters of the grinding process.

Based on the above parameters, we created a linear system model in the Matlab package and got the following result. Based on the system model, we created a predictive controller model in Matlab and created the transient responses of the system based on this model. To do this, the flow rate of the circulating mixture, the ore supplied for grinding and the feed water of the sump at the controller inlet, as well as the estimate of the particle size of the product, the total component of the mill load and the grinding volume of the sump at the controller outlet were selected. As a result of using the controller with a predictive model for a period of 0.4-0.9 min, the flow rate of the circulating mixture was 650 m^3/h, the ore supplied for grinding was 82 t/h, the sump feed water was 400 m^3/h. At the output of the system, we obtained the following values for the evaluation of the particle size of the product - 76%, the total component of the mill load - 25%, the grinding volume of the sump - 15m^3.

4 Conclusion

In conclusion, the new donation to the project involves the combination of a non-linear controller and a state estimator for the grinding circuit. This innovative approach allows for independent regulation of product quality and throughput, as well as the ability to cancel process disturbances. By utilizing a mixture of non-linear predictive model controllers and dynamic inversion, the computational costs that have previously prevented industrial applications of predictive control can be reduced. The simulation results demonstrate that the proposed approach is effective in managing the ore grinding industrial cycle, using only practical measurements. Notably, the simulation was conducted under external interference and process noise, and various performance indices were used to quantify the effect of disturbances on the grinding circuit for both controllers.

The results indicate that the predictive controller model provides independent control of product quality and throughput, and that the model predictive controller achieves better results in the presence of parametric noise and process noise, as evidenced by the computed performance functions.

References

1. I.K. Craig, I. MacLeod, Control Eng. Practice **3(5)**, 621-630 (1995)
2. H. Sh. Dang, Y. Zhang, G. Wang, Process Automation Instrumentation **04** (2014)
3. L.C. Coetzee, I.K. Craig, E.C. Kerrigan, 17th IFAC World Congr (2008)
4. K. Nageswararao, D. Wiseman, T. Napier-Munn, Minerals Eng. **17(5)** (2004)
5. D.P. Mukhitdinov, Y.B. Kadirov, I.R. Sultanov, Journal of Physics: Conference Series **2373(7)** (2022). https://www.doi.org/10.1088/1742-6596/2373/7/072025
6. N.R. Yusupbekov, D.P. Mukhitdinov, O.U. Sattarov, Intelligent Systems and Computing **1323** AISC (2021). https://www.doi.org/10.1007/978-3-030-68004-6_30
7. M. Musaev, S. Khodjaeva, A. Boboev, E3S Web of Conferences. EDP Sciences **371** (2023)
8. T.V. Botirov, S.B. Latipov, B.M. Buranov, Journal of Physics: Conference Series **2094(2)** (2021). https://www.doi.org/10.1088/1742-6596/2094/2/022052
9. I. Kalandarov, Journal of Advanced Research in Dynamical and Control Systems **12(6)**,778-792 (2022). https://www.doi.org/10.1007/978-981-16-3844-2_52
10. R.O. Muminov, G.E. Raikhanov, D.A. Kuziev, Coal **5**, 32-36 (2021). https://www.doi.org/10.18796/0041-5790-2021-5-32-36.).
11. O. Sattarov, E3S Web of Conferences **390** 03012 (2023) https://www.doi.org/10.1051/e3sconf/202339003012
12. I. Kalandarov, XIV International Scientific Conference "INTERAGROMASH 2021" 887-896 (2022). https://www.doi.org/10.1007/978-3-030-81619-3_99
13. J. Sevinov, O. Boeva, AIP Conference Proceedings **2647**, 030007 (2022)

14. N.R. Yusupbekov, D.P. Mukhitdinov, Yo.B. Kadyrov, O.U. Sattarov, A.R. Samadov, AIP Conference Proceedings **2612**, 050008 (2023). https://www.doi.org/10.1063/5.0130116
15. O.A. Jumaev, J.T. Nazarov, G.B. Makhmudov, M.T. Ismoilov, M.F. Shermuradova, Journal of Physics: Conference Series **2094(2)**, 022030 (2021)
16. O.A. Jumaev, D.S. Karpovich, G.B. Makhmudov, AIP Conference Proceedings **2656(1)**, 020026 (2022)
17. Kh.S. Bakhronov, A.A. Akhmatov, J. Chem. Technol. **29**, 442-448 (2021). https://doi.org/10.15421/jchemtech.v29i3.229656
18. O.A. Jumaev, J.T. Nazarov, R.R. Sayfulin, M.T. Ismoilov, G.B. Mahmudov, Journal of Physics: Conference Series **1679(4)**, 042037 (2020)